**Proceedings of the ASME 2010 10th Biennial Conference on Engineering Systems Design and Analysis**
**ESDA2010**
**July 12-14, 2010, Istanbul, Turkey**

**ESDA2010-24499**

# FAST AFM SCANNING WITH PARAMETER SPACE BASED ROBUST REPETITIVE CONTROL DESIGNED USING THE COMES TOOLBOX

**Serkan Necipoğlu***
Department of Mechanical Engineering
Mekar Mechatronics Research Laboratories
İstanbul Technical University, İstanbul, Turkey

**Burak Demirel**
School of Electrical Engineering
Automatic Control Laboratory
The Royal Institute of Technology (KTH),
Stockholm, Sweden

**Levent Güvenç**
Department of Mechanical Engineering
Mekar Mechatronics Research Laboratories
İstanbul Technical University, İstanbul, Turkey

## ABSTRACT

Atomic Force Microscope (AFM) is a very strong and beneficial instrument for acquiring images at nanometer scale. Hence, obtaining better image quality and scan speed is a research area of great interest. Improving the dynamic responses of the scanning probe and the vertical motion of the scanner mechanisms are the two major areas of concentration in this sense. Improving the vertical dynamics is achieved either by designing more complex scanner mechanisms with higher bandwidth or designing more sophisticated controllers rather than the PI, PID or PIID types of controllers that are mostly used in practice. In this paper, the authors focus on designing a repetitive control scheme for fast and accurate scanning. It is possible to implement repetitive control to achieve this goal when it is considered that the successive lines of the scan are quite similar due to the very small steps taken to advance on the sample. Repetitive control can reject higher frequency disturbances due to the surface topography in AFM much better than a conventional controller can, as it can drive the error caused by any periodic input signal to zero. Besides increasing the scan speed, it is also important that the phase lag can be compensated perfectly using repetitive control, with the knowledge of the surface topography from the previous period by introducing appropriate phase advance.

## 1 INTRODUCTION

The Atomic Force Microscope (AFM) which has been a fascinating invention of Binnig, Quate, and Gerber [1] is a highly beneficial instrument used for acquiring surface topography at precision of nanometers. The selective features such as the ability of fast and easy sample preparation; air, liquid, and vacuum environments of operation; relatively lower costs; etc. make it an imaging technique of strong preference. Hence, improving the performance of AFMs has been a very interesting and important goal for many scientists. The performance of an AFM can be described by the scanning speed and the image quality which are inversely proportional. The two major limitations on scanning speed without violating the image quality and stability are the transient response of the cantilever probe and the mechanical bandwidth of the mechanisms used on vertical axis "z", which are mostly made of piezoelectric actuators. These are followed by the general limitations of the feedback loop such as the time delays, sampling rate in case of digital control, facts about sensors, RMS conversion rate etc. More information on AFM dynamics and control is given in [2] and [3] for deeper understanding of the whole discussion. Fig. 1 shows a basic presentation of an AFM setup.

The transient response of the probe is quantified by the quality factor (Q) of the cantilever beam [4]. High Q values

* Author of correspondence: necipoglu@itu.edu.tr

 

cause slow response of the probe to surface topography and even instability in dynamic, amplitude modulated (AM) atomic force microscopy, e.g. tapping mode. An active Q control to improve the response time is also proposed in [4]. An adaptive Q control (AQC) depending on the surface properties is proposed in [5] where as a full state feedback control method affecting both on the Q and the resonant frequency of the vibrating probe is presented in [6].

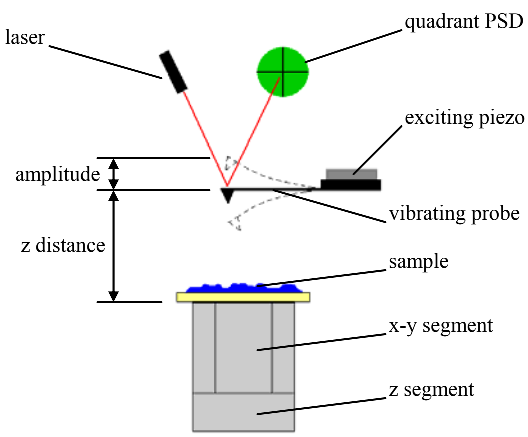


**Figure 1.** Basic AFM setup: The probe is excited by a piezoelectric element using a sinusoidal wave. The probe's deflection is measured by sensing the displacement of the laser beam reflected from the tip onto a photo sensor diode. The sample is placed on a piezotube. The upper quartered part of the piezotube is used for the raster scan motion on x-y plane and the lower single part is used for the vertical motion on z.

It is very common among the physicists to use a PI, PID, PII or a PIID controller for the vertical motion of the scanner on z direction [3]. Obviously, a simple PI controller can not improve the actuator's mechanical bandwidth to perform good surface tracking at high frequencies. Adding a derivative term seems to be a good idea at first but this is avoided since the measurement of the probe's deflection is noisy. However, the bandwidth of the scanner's vertical motion on z can be improved by more sophisticated mechanical design [7] or implementation of more sophisticated control techniques. Such a controller is implemented in [8] utilizing the $H_\infty$ theory. Sophisticated robust controllers can handle the inevitable nonlinearities and system uncertainties as well.

When the continuity of the scanned surface is considered, it is reasonable to assume that the successive lines of the scan are similar. This motivates research people to make use of the past information for improving the performance of the scan on the following lines. A combined feed-forward and $H_\infty$ controller is used in [9] for this purpose. Other feed-forward, learning and observer based controllers are proposed in [10]-[12] for the periodic motions of the scanner as well as a brief discussion about the combination of feedback and feed-forward controllers is presented in [13].

Having the same reasonable assumption made for the feed-forward controllers, this paper focuses on the repetitive control technique which is a powerful way of tracking or rejecting periodic signals [14]. The organization of the rest of the paper is as follows. In Section 2, a tapping mode AFM system scheme is introduced along with a description of the experimental AFM hardware being used. Repetitive control basics and mapping the design specifications into parameter space are explained in Sections 3 and 4, respectively. The repetitive control features of the COMES (Control of Mechatronic Systems toolbox) are outlined in Section 5. In Section 6, a parameter space based robust repetitive controller is designed using the COMES toolbox running in Matlab. Simulation results obtained using an accurate and realistic computer model are demonstrated in Section 7. The paper ends with concluding remarks in the last section.

## 2 TAPPING MODE AFM SYSTEM MODEL

We are influenced by the numerical model in [15] which is built for simulating a tapping mode AFM on computer. The complete system can be redrawn as in Fig. 2 for control purposes. The scanning probe is vibrated at a certain frequency of 221 KHz. The excitation signal is adjusted to maintain the free air amplitude of 45nm where the Q factor is set to 79. The reason to the selection of the Q will be explained shortly.

Quickly refreshing the working principles of tapping mode AFM; the interaction forces between the tip and the sample surface change the amplitude of vibration. Since it is desired to keep these forces unchanged, it is necessary to keep the amplitude of the probe's vibration unchanged. This is achieved by controlling the distance between the tip and the surface by feeding back this amplitude. This is also called the constant force scanning. It is quite reasonable to conclude from the above discussion that the probe works like a sensor of interaction forces such that the input is the distance, and the output is the amplitude of the vibration as shown in Fig. 1.

However, the probe block in Fig. 2(a) is not linear. The nonlinearities rise from the attractive and the repulsive regimes of the interaction forces, probes indentation into the sample, etc. [15]. Reader should note that all those facts are present in the model that is used for simulations here. Fortunately, we observed from the numerical simulations that the probe shows a quite linear behavior for the input signals greater that 10nm with a DC gain equal to 1, approximately. For those sizes of the inputs, the dynamics can be characterized by a first order filter due to the sharp 90 degrees phase transition observed at around 3 KHz. The nonlinearities occur such that the DC gain converges to 2 and the dynamics become oscillatory in the order of 2 for closer proximity of the tip to the surface.

We want the probe's dynamics to be involved as few as possible at this moment because we are concerned on improving the bandwidth of the scanner's vertical motion which is typically from 1 to 40 KHz. That is why the Q value is chosen to be low. Therefore, we neglect the uncertainties described in Fig. 2(c) in the linear analysis and assume a static

 

P(s) = 1 since we will be travelling in the regions satisfying that condition. Robust handling of the probe nonlinearities will be discussed another time.

Different than in [15], the stage dynamics is chosen as the one of a piezotube actuator given in [16]. It is to emphasize that faster scanning is possible using little more complex controller on simple and cheap actuators instead of using highly more complex and expensive ones. The transfer function of the piezotube's vertical motion is given in (1), where the input is the driving voltage and the output is the displacement on z axis in meters.

$$\frac{z_{pt}(s)}{V_z(s)} = \frac{158.7}{s^2 + 1328s + 1.763 \times 10^{10}} \tag{1}$$

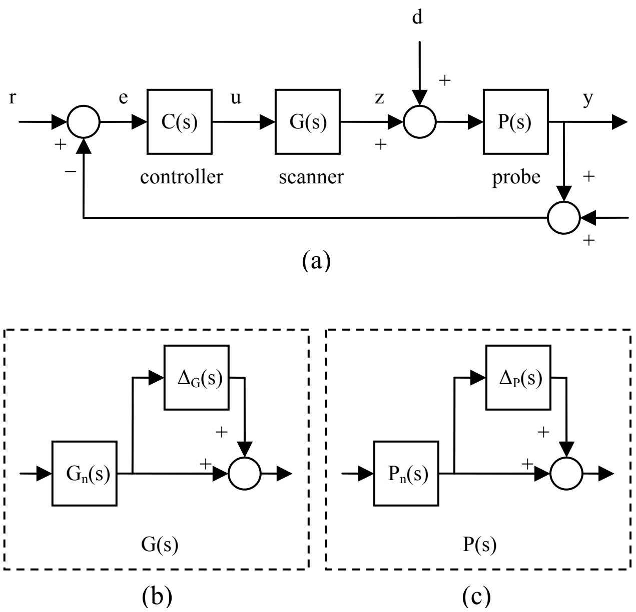


**Figure 2.** (a) AFM system model in classical control means where r is the set amplitude of the probe vibration, y is the actual amplitude, u is the control signal in volts, z is the scanner's vertical motion in nanometers, and d is the surface topography; (b) the uncertainty on the linear scanner model; and (c) the uncertainty on the linear probe model.

Reference [16] states that the model is derived by curve fitting up to the first mode resonance frequency. The higher frequencies involve uncertainties as it is most of the case when a high order system is modeled as a reduced order one.

The controller block is designed to keep the output of the feedback loop at the reference value which is the set amplitude of the probe's vibration. The amplitude is calculated by RMS conversion on each 10 oscillations of the probe. The amplitude sensor dynamics are usually in the order of MHz. So, it is contributed as a static gain in the numerical model.

It is clear from Fig. 2 that the surface topography is treated as disturbance to be rejected. The scanner's motion on z axis is recorded while performing this and so the surface topography is obtained.

We transformed the complicated AFM system in [15] into a very common and well known control problem with some assumptions made especially on the sensor probe and the piezotube actuator. This is why a robust controller is required. Then we can proceed with the linear analysis and robust design.

## 3 REPETITIVE CONTROL BASICS

The repetitive control structure is shown in Fig. 3 where $G_n$ is the nominal model of the plant, $\Delta_m$ is the normalized unstructured multiplicative model uncertainty, $W_T$ is the multiplicative uncertainty weighting function and $\tau_d$ is the period of the periodic exogenous signal. *q(s)* and *b(s)* are filters used for tuning the repetitive controller. Repetitive control systems can track periodic signals very accurately and can reject periodic disturbances very satisfactorily. This is due to the fact that the positive feedback loop in Fig. 3 is a generator of periodic signals with period $\tau_d$ for $q(s) = 1$. A low pass filter with unity DC gain is used for *q(s)* for robustness of stability [17] and [18].

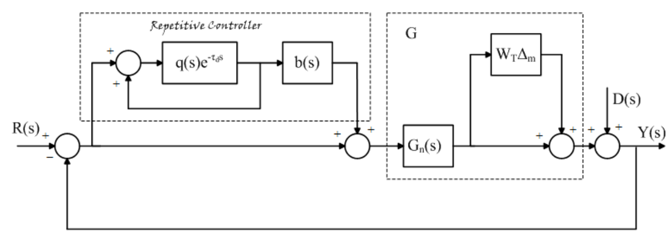


**Figure 3.** Repetitive control structure.

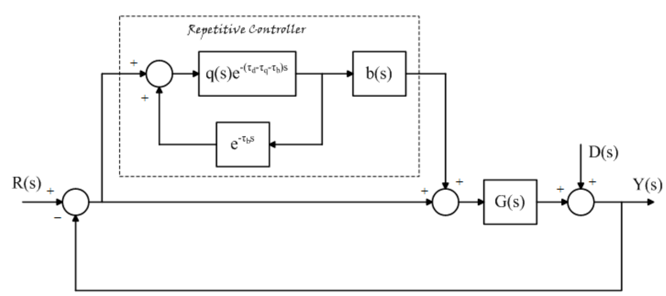


**Figure 4.** Modified repetitive control structure.

The repetitive controller design involves the design of the two filters *q(s)* and *b(s)* seen in Fig. 3. In the frequency domain, the ideal low–pass filter *q(jω)* would be 1 in the frequency range of interest and zero at higher frequencies. This is not possible and *q(jω)* will have negative phase angle which will make *q(jω)* differ from 1, resulting in reduced accuracy. So as to improve the accuracy of the repetitive controller, a small time advance is customarily incorporated into *q(s)* to cancel out the negative phase of its low–pass filter part within its bandwidth. This small time advance can easily be absorbed by the much larger time delay $\tau_d$ corresponding to the period of the exogenous input signal and does not constitute an implementation problem (see Fig. 4).

The main objective of the usage of the dynamic compensator *b(s)* is improving the relative stability, the transient response and the steady state accuracy in combination with the low–pass filter *q(s)*. Consider the function of frequency given by

$$R(\omega)=\left|q(j\omega)\left[1-b(j\omega)\frac{G(j\omega)}{1+G(j\omega)}\right]\right| \tag{2}$$

which is called the regenerative spectrum in [19]. According to the same reference, *R(ω)*<1 for all ω is a sufficient condition for stability. Moreover, *R(ω)* can be utilized to obtain a good approximation of the locus of the dominant characteristic roots of the repetitive control system for large time delay, thus resulting in a measure of relative stability, as well. Accordingly, the compensator *b(s)* is designed to approximately invert *G/(1+G)* within the bandwidth of *q(s)* in an effort to minimize *R(ω)*. The dynamic compensator *b(s)* can be selected as only a small time advance or time advance multiplied by a low–pass filter in order to minimize *R(ω)*. In order to make *R(ω)*<1, the time advance in the filter *b(s)* is chosen to cancel out the negative phase of *G/(1+G)*. This small time advance can easily be absorbed by the much larger time delay $\tau_d$ corresponding to the period of the exogenous input signal and does not constitute an implementation problem (see Fig. 4).

The *q(s)* and *b(s)* filters are thus expressed as

$$q(s)=q_p(s)e^{\tau_q s} \tag{3}$$

$$b(s)=b_p(s)e^{\tau_b s} \tag{4}$$

The time advances $\tau_q$ and $\tau_b$ are firstly chosen to decrease the magnitude of *R(ω)* given in Eq. (2). Then, the design focuses on pairs of chosen parameters in $q_p(s)$ or $b_p(s)$ to satisfy a frequency domain bound on the mixed sensitivity performance criterion. If $L$ denotes the loop gain of a control system, its sensitivity and complementary sensitivity transfer functions are

$$S:=\frac{1}{1+L} \tag{5}$$

$$T:=\frac{L}{1+L} \tag{6}$$

The parameter space design, aims at satisfying the mixed sensitivity performance requirement

$$\left\| |W_S S|+|W_T T| \right\|_\infty <1 \quad \text{or} \quad |W_S S|+|W_T T|<1 \quad \text{for } \forall\omega \tag{7}$$

where $W_S$ and $W_T$ are the sensitivity and complementary sensitivity function weights. The loop gain of the repetitive control system seen in Figs. 3 and 4 are given by

$$L=G\left(1+\frac{q_p}{1-q_p e^{(-\tau_d+\tau_q)s}}b_p e^{(-\tau_d+\tau_q+\tau_b)s}\right) \tag{8}$$

The mixed sensitivity design requires

$$\begin{aligned}&|W_S(\omega)S(j\omega)|+|W_T(\omega)T(j\omega)|=\\ &\qquad\left|\frac{W_S(\omega)}{1+L(j\omega)}\right|+\left|\frac{W_T(\omega)L(j\omega)}{1+L(j\omega)}\right|<1\end{aligned} \tag{9}$$

*or equivalently* Eq. (10) to be satisfied for all ω.

$$|W_S(\omega)|+|W_T(\omega)L(j\omega)|<|1+L(j\omega)| \tag{10}$$

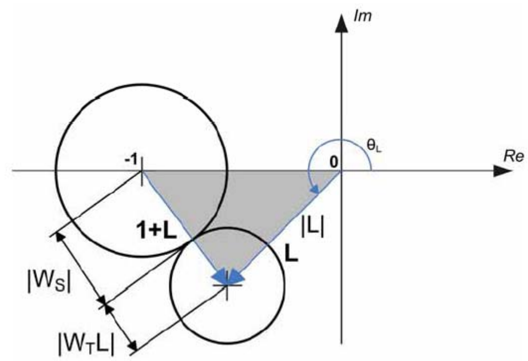


**Figure 5.** Illustration of the point condition for the mixed sensitivity.

## 4 MAPPING MIXED SENSITIVITY SPECIFICATIONS INTO CONTROLLER PARAMETER SPACE

A repetitive controller design procedure based on mapping the mixed sensitivity frequency domain performance specification given in Eq. (10) with an equality sign into the chosen repetitive controller parameter plane at a chosen frequency is described.

Consider the mixed sensitivity problem given in Fig. 5 illustrating Eq. (10) with an equality sign (called the mixed sensitivity point condition). Apply the cosine rule to the triangle with vertices at the origin, -1 and $L$ in Fig. 5 to obtain

$$\left(|W_S(\omega)|+|W_T(\omega)L(j\omega)|\right)^2=|L(j\omega)|^2+1^2+2|L(j\omega)|\cos\theta_L \tag{11}$$

Equation (11) is quadratic in $|L(j\omega)|$ and its solutions are

$$\left|L(j\omega)\right| = \frac{\left(-\cos\theta_L + \left|W_S(\omega)\right|\left|W_T(\omega)\right|\right) \pm \sqrt{\Delta_M(\omega)}}{1-\left|W_T(\omega)\right|^2} \tag{12}$$

where

$$\Delta_M(\omega) = \cos^2\theta_L + \left|W_S(\omega)\right|^2 + \left|W_T(\omega)\right|^2 - 2\left|W_S(\omega)\right|\left|W_T(\omega)\right|\cos\theta_L - 1 \tag{13}$$

Only, positive and real solutions for $|L|$ are allowed, i.e., $\Delta_M \geq 0$ in Eq. (12) must be satisfied. A detailed explanation of the point condition solution is given in [20].

## 5 REPETITIVE CONTROL FEATURES OF COMES

COMES (Control of Mechatronic Systems) toolbox is a GUI (Graphical User Interface) for the routines of four different control approaches [21]: classical control (lead, lag, PID etc.), preview control, model regulator control and repetitive control, which are coded in Matlab M-files. The repetitive control design module of COMES toolbox is used for determining the parameter space regions corresponding to chosen frequency-domain criteria. The technique behind it is based on mapping a frequency domain mixed sensitivity bound into the chosen repetitive controller parameter plane as explained in section 4. The procedure leads to graphical solution regions in 2-D plots for each design specification. A screenshot from the repetitive control design module of COMES is shown in Fig. 6.

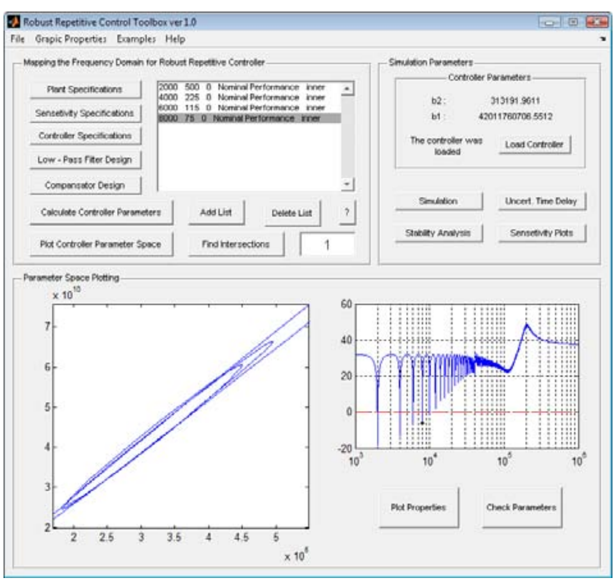


**Figure 6.** GUI of the repetitive control module of COMES.

First, the plant specifications are introduced. Second, the sensitivity and complementary sensitivity weights are introduced for a certain frequency chosen from the predefined design criteria. Then the controller specifications such as the fundamental or the harmonics of the repetitive signal and the number of grids for $\theta$ sweep in Fig. 5 are entered. The $q$ filter, which is a second order low-pass as described in section 3, is entered parametrically in terms of $a_{00}$ and $a_{01}$ to be calculated. Then the compensator $b$ is entered as in section 3 as well. Finally, the low pass parameters are calculated numerically by COMES using the technique given in section 4 and the solution region satisfying the design criteria is plotted in the parameter space. Having repeated this calculation by updating the sensitivity specifications and the controller specifications for each frequency, new solution regions are plotted on the same plane. The overall solution satisfying all the design criteria is the intersection of these regions which is shown color filled. The $q$ filter parameters must be chosen from that region as a result.

The frequency plots of sensitivity, complementary sensitivity, loop gain and the regeneration spectrum can be observed for convenience using the 'Sensitivity Plots' pane. Obviously, the aim of the COMES is to provide a user-friendly toolbox utilized with a GUI which runs all the work behind automatically. Hence, the user can focus on analyzing the graphical results rather than doing all the complicated calculations.

## 6 ROBUST REPETITIVE CONTROLLER DESIGN USING THE COMES TOOLBOX

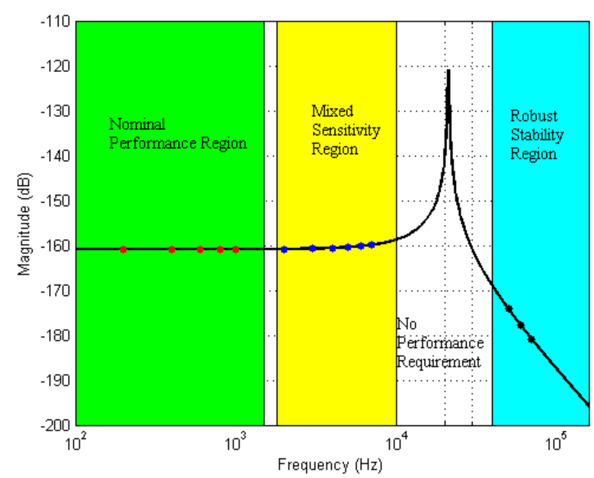


**Figure 7.** Design specifications for the repetitive controller.

The point condition solution discussed in Section 4 is implemented using the repetitive control module of the COMES toolbox. The design specifications are determined as in Fig. 7, such that good tracking (nominal performance) is required at low frequencies, mixed sensitivity is required at intermediate frequencies, and robust stability is required at high frequencies due to the unstructured multiplicative uncertainties of the piezotube. No performance is required near the resonance since it is not operated at those frequencies.

The weights $W_S$ and $W_T$ are determined for arbitrary frequencies inside the regions in Fig. 7 as shown in Table 1. The design is based on periodic signals at 200Hz, hence the repeating period is 0.005 seconds.

**Table 1.** Weights for Controller Design

| $f=k/\tau_d$ (Hz) | $k$ | $W_S$ | $W_T$ |
|---|---|---|---|
| 200 | 1 | 500 | 0 |
| 400 | 2 | 250 | 0 |
| 600 | 3 | 115 | 0 |
| 800 | 4 | 60 | 0 |
| 1000 | 5 | 40 | 0 |
| 3000 | 15 | 3 | 0.02 |
| 4000 | 20 | 1.9 | 0.02 |
| 5000 | 25 | 1.45 | 0.02 |
| 6000 | 30 | 1.25 | 0.05 |
| 7000 | 35 | 1.1 | 0.05 |
| 50000 | 250 | 0 | 0.2 |
| 60000 | 300 | 0 | 0.2 |
| 70000 | 350 | 0 | 0.2 |

$\tau_d$ = 0.005 which is the period of the repetitive signal.

Having determined the design specifications in Table 1, the filter *b(s)* is designed as in (14), as it was explained in section 3, and *q(s)* is chosen to be in the form of (15). The parameters $a_{00}$ and $a_{01}$ in (15) must be appropriately selected from the parameter space to satisfy the design specifications given in Fig. 7 and Table 1. The solution regions of the point condition on the parameter space are plotted in Fig. 8 for each frequency given in Table 1. The intersection of those regions is color filled and an arbitrary point somewhere near the centre of this intersection is selected to determine $a_{00}$ and $a_{01}$ that are given in (16).

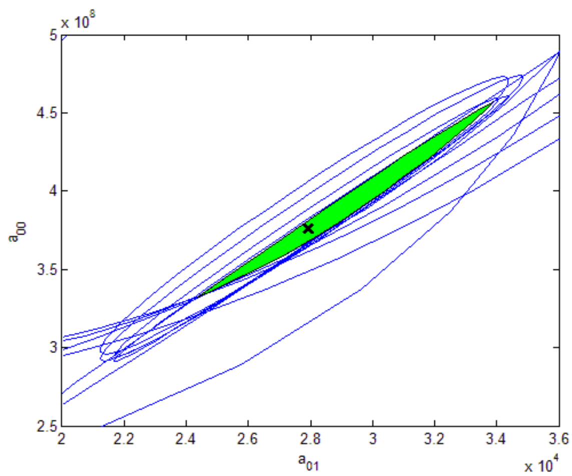


**Figure 8.** Solution regions of the point condition.

$$b(s)=\frac{6.707\times10^{7}s^{2}+1.591\times10^{14}s+1.104\times10^{18}}{s^{2}+2\times10^{5}s+10^{10}} \qquad (14)$$

$$q(s)=\frac{a_{00}}{s^{2}+a_{01}s+a_{00}} \qquad (15)$$

$$a_{00}=3.8882\times10^{8} \quad ; \quad a_{01}=2.9133\times10^{4} \qquad (16)$$

Finally, time advances $\tau_b$=6.268×10-6s and $\tau_q$=7.5×10-5s are calculated to compensate the phase lags introduced by the *q(s)* and *b(s)G(s)/[1+G(s)]* as shown in Fig. 9.

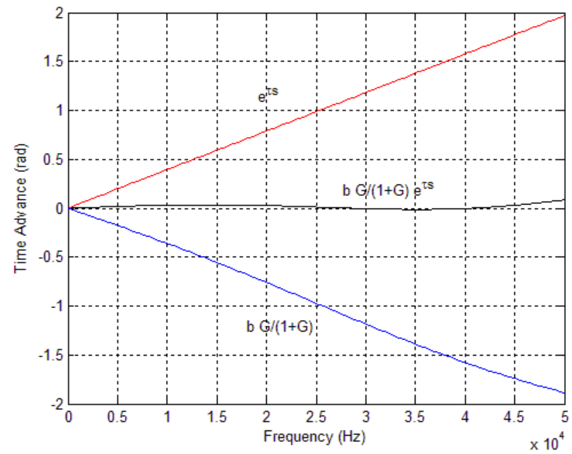


**Figure 9.** Compensation of the phase lag by time advance.

## 7 SIMULATION RESULTS

Numerical simulations are carried on as mentioned in section 2. Steps of 40 nanometers height at 200Hz is assumed to be the surface topography to scan. The result obtained using a well tuned PI controller for the vertical motion of the piezotube is illustrated in Fig. 10(a) where as the error is shown in Fig. 10(b).

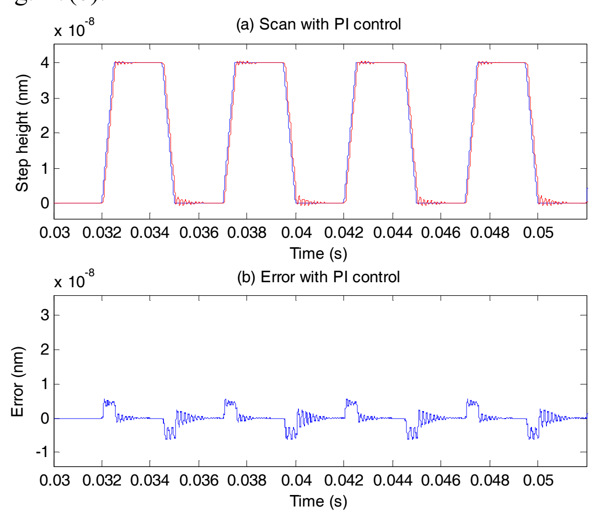


**Figure 10.** (a) is the illustration of the scan with PI control and (b) is the error on the probe's oscillation amplitude.

Fig. 11(a) illustrates the scan simulation under repetitive controller instead of the PI and the error is shown in Fig. 11(b). Apparently, the scan obtained with the repetitive controller is better than the PI after the first two periods. The error is smaller at the moments of disturbances and so is the control effort as a consequence.

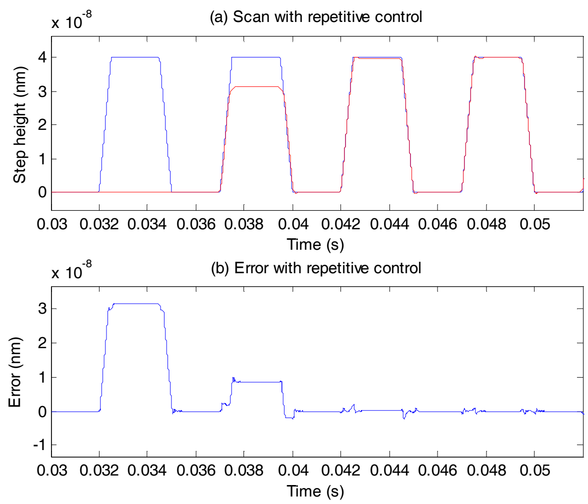


**Figure 11.** (a) is the illustration of the scan with repetitive control and (b) is the error on the probe's oscillation amplitude.

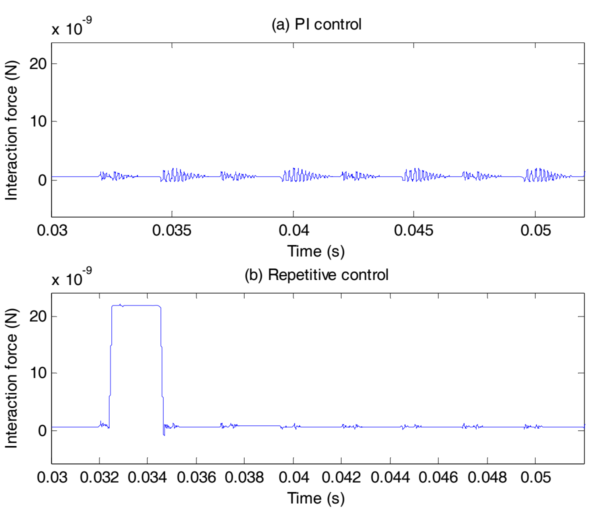


**Figure 12.** (a) is the illustration of the interaction forces in the case of PI control and (b) is the illustration of the same forces in the case of repetitive control.

Another important fact of constant force scanning is the size of the interaction forces between the probe's tip and the sample surface. Big forces are not convenient in order to avoid the probable damages on the tip and the sample, especially when the sample is an organic matter like a biological specimen. The comparison of the interaction forces with the PI and the repetitive controller are demonstrated in Fig. 12. After the first period, the forces are reduced considerably both on the flat parts of the steps and at the moments of disturbances when more control effort is needed.

## 8 CONCLUSION AND FUTURE WORK

The repetitive controller can reject the disturbances at higher frequencies when compared to the PI controller and hence provide faster and better scan of the surface topography, maintaining small forces on the tip and the sample. This is a result of the extended bandwidth of the control system on the z axis of vertical motion which is introduced by the repetitive controller. The delayed response of number of periods is inevitable. This is a handicap when the periodic signal is subjected to variations. However, perfect tracking is obtained after one period delay when these variations are small and smooth. Besides, it is not a drawback for the use of repetitive controller when the number delay period is known which can be corrected computationally after acquisition because higher image resolution at fast scan rates is desired primarily.

The repetitive controller is designed as an "add on structure" through the forward path as shown in Fig. 3. It is usually operated with a conventional controller, e.g. PID, connected in parallel or serial. In case the input signal is not periodic, the repetitive controller can be turned off.

Experimental work is being carried on a real AFM system with repetitive controller in our labs. The improvements on the scan performance supporting the idea here are going to be presented shortly.

## REFERENCES

[1] Binnig, G. K., Quate, C. F., and Gerber, C., 1986, "Atomic force microscope," Physical Review Letters, **56**, pp. 930-933.

[2] Garcia, R., and Perez, R., 2002, "Dynamic Atomic Force Microscopy Methods," Elsevier Science B.V., Surface Science Reports **47**, pp. 197-301.

[3] Abramovitch, D. Y., Andersson, S. B., Pao, L. Y., and Schitter, G., 2007, "A Tutorial on the Mechanisms, Dynamics, and Control of Atomic Force Microscopes," in *Proc. American Control Conference,* New York City, USA.

[4] Sulchek, T., Yaralioglu, G. G., and Quate, C. F., 2002, "Characterization and Optimization of Scan Speed for Tapping-mode Atomic Force Microscopy," Review of Scientific Instruments, **73**, (8), American Institute of Physics.

[5] Gunev, I., Varol, A., Karaman, S., and Basdogan, C., 2007, "Adaptive Q Control for Tapping Mode Nanoscanning Using a Piezoactuated Bimorph Probe," Review of Scientific Instruments, **78**, 043778, American Institute of Physics.

[6] Orun, B., Necipoglu, S., Basdogan, C., Guvenc, L., 2009, "State Feedback Control for Adjusting the Dynamic Behavior of a Piezo-actuated Bimorph AFM Probe,"

Review of Scientific Instruments, **80**, (1), American Institute of Physics.

[7] Schitter, G., Aström, K. J., DeMartini, B. E., Thurner, P. J., Turner, K. L., and Hansma, P. K., 2007, "Design and Modeling of a High-speed AFM Scanner," IEEE Transactions on Control Systems Technology, **15**, (5) , IEEE.

[8] Schitter, G., Menold, P., Knapp, H. F., Allgöwer, F., and Stemmer, A., 2001, "High Performance Feedback for Fast Scanning Atomic Force Microscopes," Review of Scientific Instruments, **72**, (8), American Institute of Physics.

[9] Schitter, G., Allgöwer, F., and Stemmer, A., 2004, "A New Control Strategy for High-speed Atomic Force Microscopy," Institute of Physics Publishing, Nanotechnology, **15**, pp. 108-114.

[10] Li, Y., and Bechhoefer, J., 2008, "Feedforward Control of a Piezoelectric Flexure Stage for AFM" in *Proc. American Control Conference,* Seattle, Washington, USA.

[11] Fujimoto, H., and Oshima, T., 2008, "Nanoscale Servo Control of Contact-mode AFM with Surface Topography Learning Observer," *10th IEEE International Workshop on Advanced Motion Control,* pp. 568-573.

[12] Salapaka, S. M., De, T., and Sebastian, A., 2005, "A Robust Control Based Solution to the Sample-profile Estimation Problem in Fast Atomic Force Microscopy," International Journal of Robust and Nonlinear Control, **15**, pp. 821-837.

[13] Pao, L. Y., Butterworth, J. A., and Abramovitch, D. Y., 2007, "Combined Feedforward/Feedback Control of Atomic Force Microscopes," in *Proc. American Control Conference,* New York City, USA.

[14] Aksun Guvenc, B., Guvenc, L., 2006, "Robust Repetitive Controller Design in Parameter Space," ASME Journal of Dynamic Systems, Measurement and Control, **128**, (2), pp. 406-413.

[15] Varol, A., Gunev, I., Orun, B., and Basdogan, C., 2008, "Numerical Simulation of Nano Scanning in Intermittent-Contact Mode AFM Under Q Control," Nanotechnology, (19).

[16] Ohara, T., and Youcef-Toumi, K., 1995, "Dynamics and Control of Piezotube Actuators for Subnanometer Precision Applications," in *Proc. American Control Conference,* Seattle, Washinton, USA.

[17] Hara, S., Yamamoto, Y., Omata, T., and Nakano, M., 1988, "Repetitive Control Systems: A new Type Servo System for Periodic Exogenous Signals," IEEE Transactions on Automatic Control, **33**, pp. 657–667.

[18] Weiss, G., 1997, "Repetitive Control Systems: Old and New Ideas," *Systems and Control in the 21st Century*, C. Byrnes, B. Datta, D. Gilliam and C. Martin, eds., PSCT, Birkhäuser, Boston, **22**, pp. 389-404.

[19] Srinivasan, K., and Shaw, F. R., 1991, "Analysis and Design of Repetitive Control Systems Using the Regeneration Spectrum," ASME Journal of Dynamical Systems, Measurement and Control, **113**, pp. 216-222.

[20] Demirel, B., and Guvenc, L., "Parameter Space Design of Repetitive Controllers for Satisfying a Mixed Sensitivity Performance Requirement," IEEE, Transactions on Automatic Control, submitted for publication.

[21] Demirel, B., 2009, "Interactive Computer-Aided Controller Design for Mechatronic Systems," M.S. Thesis, Istanbul Technical University, Istanbul, Turkey.